



Cite this: *Nanoscale*, 2024, **16**, 20067

Received 15th April 2024,  
Accepted 22nd September 2024

DOI: 10.1039/d4nr01638f

rsc.li/nanoscale

# Nucleic acid detection with single-base specificity integrating isothermal amplification and light-up aptamer probes†

Jaekyun Baek,<sup>a,c</sup> Jihyun Park<sup>b</sup> and Youngeun Kim  <sup>a,b,c</sup>

**We report a novel platform for label-free nucleic acid detection using isothermal amplification and light-up aptamer probes. This assay converts double-stranded amplicons into single-stranded targets to enable sequence-specific hybridization with split dapoxyl aptamer probes, offering attomolar sensitivity and single-base specificity.**

Nucleic acid detection, a technique that analyzes the presence of genetic materials (DNA or RNA) with specific sequences, has been utilized as an indispensable tool in a wide range of real-life applications including food safety,<sup>1</sup> environmental

monitoring,<sup>2</sup> and medical diagnostics.<sup>3</sup> Programmable and precise control to edit or functionalize nucleic acid strands has continuously evolved,<sup>4,5</sup> adding to the fundamental knowledge on molecular diagnostics, which has experienced an unprecedented pace of development during the SARS-CoV-2 pandemic.<sup>6</sup> Particularly, quantitative polymerase chain reaction (qPCR)<sup>7</sup> has revolutionized the field of nucleic acid diagnostics due to its ability to amplify, detect, and quantify specific DNA sequences in real-time, offering high sensitivity and wide applicability. However, qPCR is heavily reliant on thermocycling to facilitate exponential amplification of nucleic acids, and iteratively adjusting reaction temperatures is a time-consuming process that requires a dedicated thermocycler. As a result, the exhaustive and laborious protocol along with the demand for costly devices make qPCR more difficult to be used in decentralized settings.<sup>8</sup>

To address such limitations, isothermal amplification methods emerged as an alternative.<sup>9–11</sup> In general, isothermal methods initiate and expedite amplification at a constant

<sup>a</sup>Interdisciplinary Program in Bioengineering, Seoul National University, Seoul 08826, Republic of Korea. E-mail: youneunkim@snu.ac.kr

<sup>b</sup>Department of Materials Science and Engineering, Seoul National University, Seoul, 08826, Republic of Korea

<sup>c</sup>Research Institute of Advanced Materials, Seoul National University, Seoul, 08826, Republic of Korea

† Electronic supplementary information (ESI) available. See DOI: <https://doi.org/10.1039/d4nr01638f>



**Jaekyun Baek**

*Jaekyun Baek is currently a second-year master's student in the Interdisciplinary Program in Bioengineering at Seoul National University. He received the National Scholarship for Science and Engineering from 2020 to 2022. His previous and ongoing research focuses on stimuli-responsive nanomaterials, programmable biomaterials, and biosensor development. Based on these interests, he worked as a research intern at the Sensor*

*System Research Center, Korea Institute of Science and Technology (KIST), in 2022, and has been a graduate researcher in Prof. Youngeun Kim's lab since January 2023.*



**Jihyun Park**

*Jihyun Park is a third-year undergraduate student in the Department of Materials Science and Engineering at Seoul National University. She is a Korean Presidential Science Scholarship recipient in Chemistry since 2022. Her research interests are in biosensors, drug delivery, and DNA-based materials. Based on these interests, she has worked as an undergraduate intern in Prof. Youngeun Kim's research group since January 2024.*

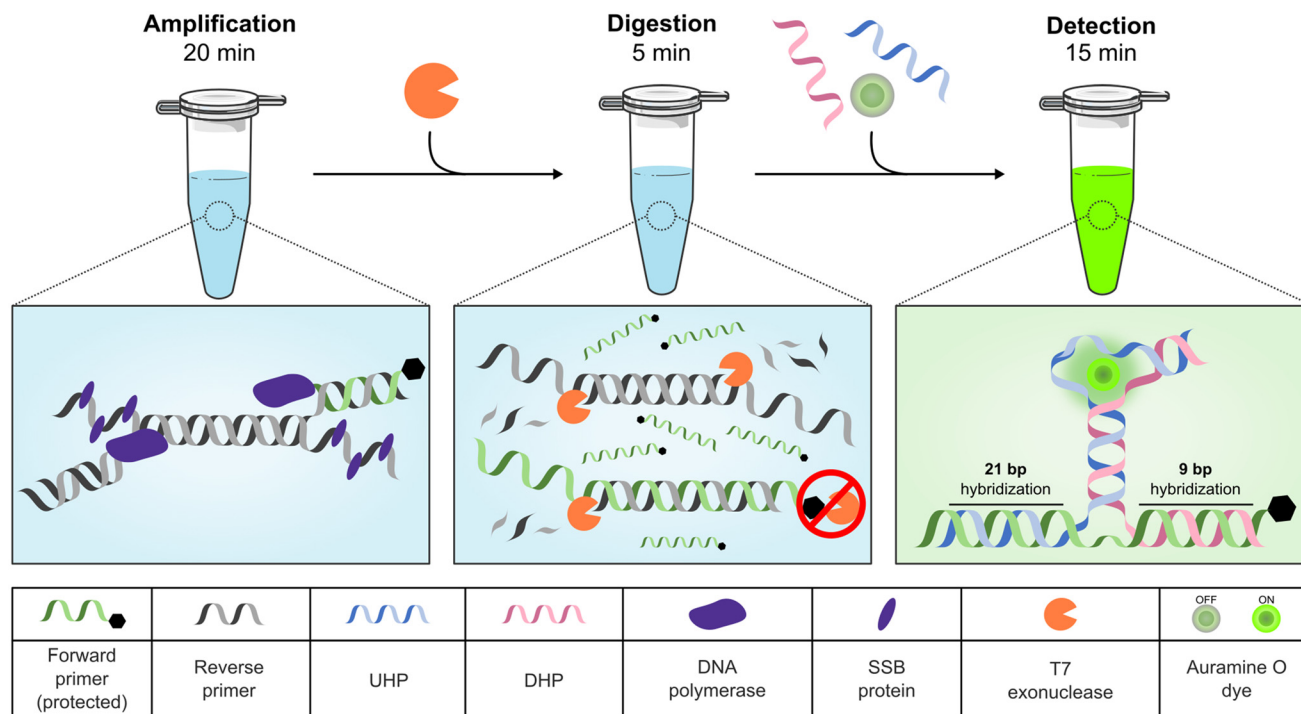


**Fig. 1** Schematic representation of CLASSIC. CLASSIC consists of three distinct reactions: amplification, digestion, and detection. Target DNA is exponentially amplified through recombinase polymerase amplification. Effectively, only the target DNA strand synthesized from the forward primer (green) that has pt modifications (black hexagon) remains intact after the enzymatic digestion. As a result, a pair of SDA probes (UHP and DHP) hybridizes to the single-stranded target and forms an aptameric core, leading to a dramatic enhancement in AO fluorescence.

temperature by the aid of nucleic acid-specific enzymes and/or unique primer pairs.<sup>12</sup> While the isothermal amplification techniques offer mild operation temperatures and relatively faster kinetics, they face challenges associated with reduced sequence specificity or non-specific amplification, leading to higher error rates.<sup>13</sup> Mitigating these errors requires either optimizing the amplification process to enhance fidelity or developing detection methods that bolster the reduced speci-

ficity. Though attempts have been made (machine learning-based primer design,<sup>14</sup> CRISPR-based sequence control,<sup>15</sup> optimized dye selection,<sup>16</sup> *etc.*) to enhance precision and minimize errors, finding a delicate balance between speed and precision in isothermal amplification techniques remains a challenge.

Herein, we demonstrate a novel nucleic acid detection platform based on isothermal amplification and split aptameric probe-based detection by including an intermediate single-strand conversion process. Combination of Light-up Aptameric probes for high Specificity and Sensitivity with Isothermal amplification and single-strand Conversion (CLASSIC) involves a three-step reaction: amplification (20 min), enzymatic digestion (5 min), and split dapoxyl aptamer (SDA)-based detection (15 min).

During amplification, a double-stranded target is amplified through recombinase polymerase amplification (RPA).<sup>17</sup> T7 exonuclease digestion step follows to keep only the successfully polymerized DNA strands to be left over after the enzymatic digestion. All but protected DNA double-stranded amplicons are digested from the 5' to 3' direction by T7 exonuclease.<sup>18</sup> The forward primer is modified with phosphorothioate (pt) bonds at its 5' end to protect against T7 exonuclease digestion,<sup>19,20</sup> and therefore mis-amplified products are enzymatically eliminated while the successfully polymerized and protected single-stranded amplicons of the target are left at the end of the digestion step.<sup>19,21</sup> Afterwards, split aptameric probes hybridize to the resulting single-stranded target and form an auramine O (AO)-



**Youngun Kim**

*Youngun Kim is an assistant professor at Seoul National University in the Department of Materials Science and Engineering. She completed her Ph.D. in Materials Science and Engineering, then worked as a postdoctoral scholar at the Wyss Institute (Harvard University) before she started at Seoul National University in 2022. She was selected as one of the "Young Innovators Under 35" by MIT Technology Review in biotechnology and medicine. Her research interests include DNA nanotechnology, nanoparticles, and biosensors.*

binding core structure, enhancing the fluorescence of AO only when the single-strand target is successfully and properly produced in the preceding process (Fig. 1).

In this work, we demonstrate CLASSIC can take advantage of each step – a rapid and easy isothermal amplification process, a simple double-stranded amplicon to single-strands conversion process, and a sequence-specific fluorescence detection process.

The *katG* gene in *Mycobacterium tuberculosis* encodes catalase-peroxidase, an enzyme crucial for the bacterium's ability

to detoxify reactive oxygen and nitrogen species, which helps it survive within the host's immune system.<sup>22</sup> In this work, we chose to detect the *katG* gene via CLASSIC, and inspired by Connelly's work,<sup>23</sup> SDA probes targeting the *katG* gene from *M. tuberculosis* were designed. Two hybridization oligonucleotide probes, upstream hybridization probe (UHP) and downstream hybridization probe (DHP), were produced by splitting the DAP-10-42 aptamer into two halves. Both probes consist of two segments: (1) a target-binding arm that selectively hybridizes to a single-stranded DNA target, and (2) a

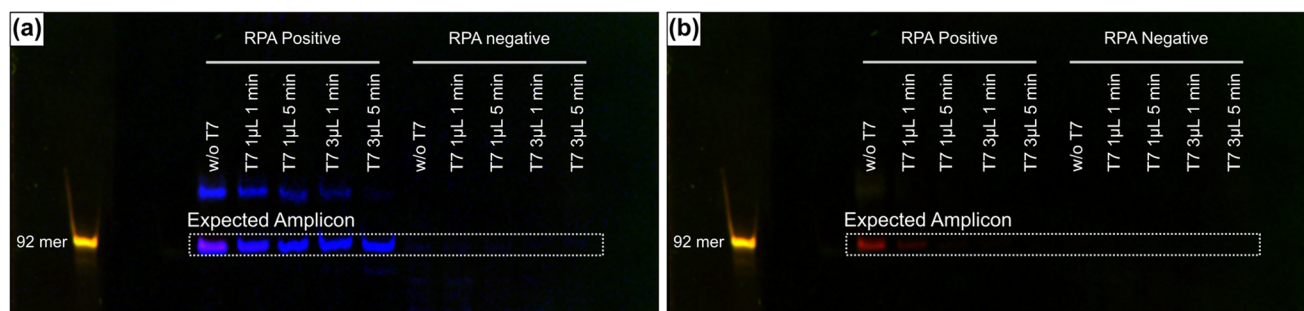


**Fig. 2** The production of single-stranded target DNA through RPA and T7 exonuclease digestion is characterized via 10% denaturing urea-PAGE. (a) Only forward primer-derived, single-stranded targets remain after digestion, as shown in the Cy5 channel (blue). (b) All reverse primer-derived amplicons were digested, as indicated by the Cy3 channel (red). Size marker oligos (92 mer) were stained with SYBR gold (yellow) as reference.

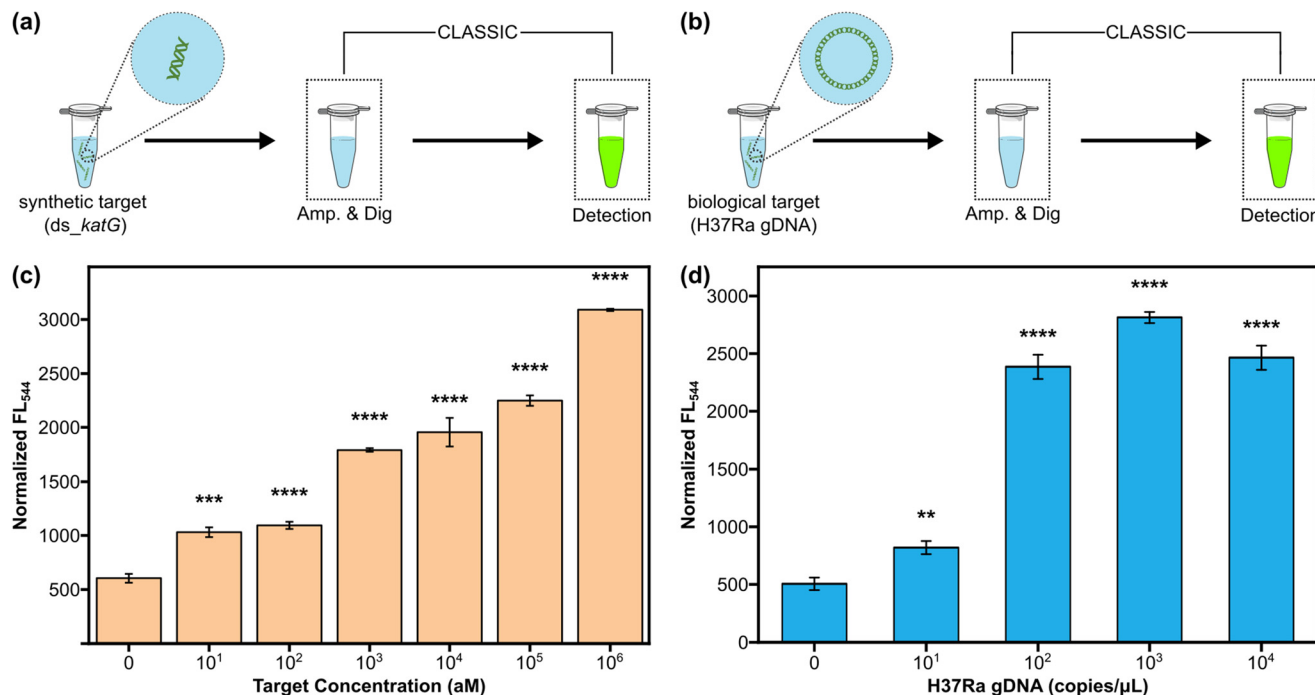


**Fig. 3** Graphical illustrations of the experiments to determine sensitivity of CLASSIC with: (a) synthetic double-stranded *katG* gene fragment, and (b) genomic DNA (gDNA) of *Mycobacterium tuberculosis* H37Ra strain. (c) Sensitivity of CLASSIC for synthetic *katG* DNA. The bar plot shows the mean (light orange)  $\pm$  standard deviation (error bar) of the normalized AO fluorescence values at specified concentrations of the synthetic *katG* strand. (d) Sensitivity of CLASSIC for H37Ra strain gDNA. The bar plot shows the mean (cyan)  $\pm$  standard deviation (error bar) of the normalized AO fluorescence signals at specified copy numbers of H37Ra gDNA. All data were obtained from three independent measurements (two-sided Student's *t*-test; \*\*,  $p < 0.01$ , \*\*\*,  $p < 0.001$ , \*\*\*\*,  $p < 0.0001$ ;  $n = 3$ ).

signal-transducing element that forms the AO-binding aptameric core and switches on the AO fluorescence. Worth of note, the target-binding arm of UHP is relatively short (9 nt) in length to discriminate a single-base mismatch,<sup>24</sup> while DHP has a longer target-binding arm (21 nt) designed to unzip the secondary structure of the target. Additionally, the 5' ends of UHP and DHP included five consecutive pt modifications, through which the probes become resistant to T7 exonuclease-mediated degradation.

Initially, the double-strand to single-strand conversion of RPA amplicons *via* T7 exonuclease digestion was confirmed *via* 10% denaturing urea-PAGE. Forward and reverse primers were independently labelled with different fluorophores (Cy5 and Cy3, respectively) to readily analyze amplified and digested products. It is worth noting that only the forward primers are protected with pt modifications at the 5' end to enable (i) nuclease resistance for forward primer-derived amplicons and (ii) selective removal of reverse primer-derived strands. The expected amplicon products were observed near 92 nt in both Cy5 and Cy3 channels, confirming successful amplification of the target ("RPA positive, w/o T7" in Fig. 2(a) and (b)). For T7 exonuclease-treated samples, Cy5-labelled amplicon bands remain at 92 nt (Fig. 2(a)) while Cy3-labelled bands are less visible or disappear (Fig. 2(b)). These results validate single-stranded target formation through comprehensive steps of RPA amplification and T7 exonuclease digestion.

The sensitivity of CLASSIC was assessed by analyzing synthetic version of *katG* analogue (ds\_*katG*) (Fig. 3(a)). Varying concentrations of ds\_*katG* ranging from 100 zM to 1 pM were tested. The results demonstrated that CLASSIC could successfully detect the synthetic target down to 10 aM (Fig. 3(c) and Fig. S4(a)† for below 10 aM). Additionally, the sensitivity of CLASSIC was further tested by using genomic DNA (gDNA) extracted from *M. tuberculosis* H37Ra strain. gDNA samples were subjected to CLASSIC at concentrations ranging from 1 to 10<sup>4</sup> copies per  $\mu$ L (Fig. 3(b)). The data suggested that CLASSIC effectively amplified and detected gDNA down to 10 copies per  $\mu$ L (Fig. 3(d)), with no detection achieved below this threshold (Fig. S4(b)†). Overall, CLASSIC was demonstrated to rapidly detect clinically relevant biological target with high sensitivity.

Sequence-specificity of CLASSIC was tested using double-stranded DNA targets with three different sequence variations at the UHP-targeted region, including: (1) a perfect match (ds\_*katG* as positive control), (2) a single-base mismatch (G to C substitution, ds\_*G > C*), and (3) a 3-base mismatch (consecutive three bases (GCG) replaced with an A or a T nucleotide, ds\_WWW). All three target samples were separately processed through the entire CLASSIC workflow, from amplification to detection (Fig. 4(a)). Denaturing urea-PAGE analysis indicated that all samples were amplified and digested to produce single-stranded targets (Fig. S4(c)†). However, CLASSIC assay results confirmed that only the perfectly matched target (ds\_*katG*) produced significant AO fluorescence as verified *via* statistical analysis (Fig. 4(b)). The mismatched targets (ds\_*G > C* and ds\_WWW) generated AO fluorescence signals that were similar to that of NC. Collectively, these results proved that

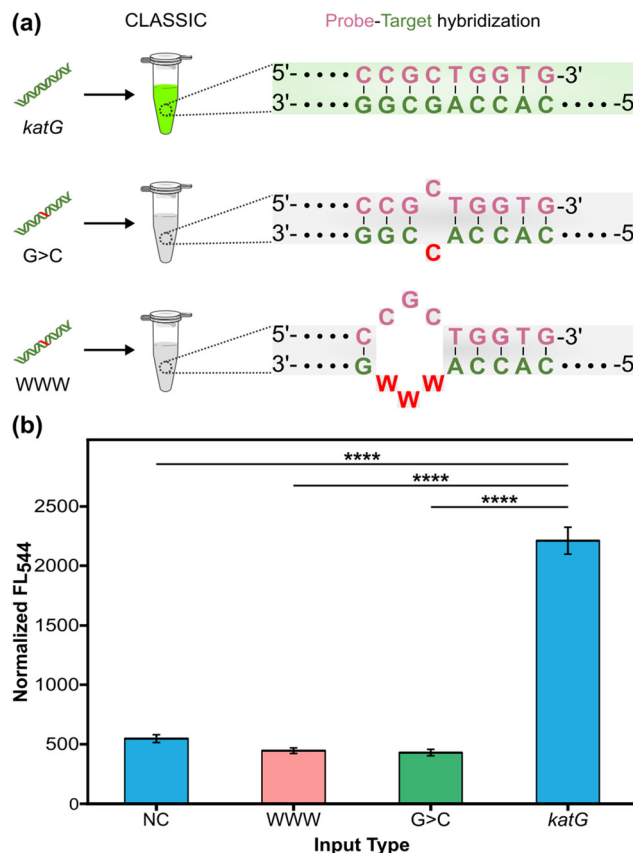


**Fig. 4** (a) Schematic of the experiment to verify the specificity of CLASSIC. Three samples (ds\_*katG*, ds\_*G > C*, and ds\_WWW) were tested via CLASSIC independently at an initial concentration of 10 pM. ds\_*G > C* has a single-base substitution (G to C) and ds\_WWW has a continuous three-nucleotide change from *katG*. (b) Single-base specificity of CLASSIC. The bar plot displays the mean and standard deviation (error bar) of normalized AO fluorescence from samples. While *katG* (cyan) exhibited a significant increase in AO fluorescence, the mismatched target samples showed signals similar to that of the negative control. Fluorescence data were obtained from four independent measurements (two-sided Student's *t*-test; \*\*\*\*:  $p < 0.0001$ ;  $n = 4$ ).

CLASSIC was able to differentiate base mismatches at the single-nucleotide level, showcasing remarkable sequence-specificity of the split probe system.

In conclusion, we developed a label-free DNA detection platform capable of discriminating a single-nucleotide difference by combining a split aptameric sensing step with isothermal amplification and single-strand conversion steps. The key to CLASSIC is to systemically mitigate the likelihood of false positive signals generated from non-specific amplicons by employing two comprehensive steps after amplification: single-strand conversion (digestion) followed by sequence-specific detection. CLASSIC enables sensitive detection of the target DNA as low as 10 aM (*katG* gene fragment) and 10 copies per  $\mu$ L (gDNA from *M. tuberculosis* H37Ra strain) within 45 minutes with extremely high sequence-specificity capable of discriminating single-nucleotide variations. This work is the first approach to embody the detection of a double-stranded DNA target with a



split aptameric sensor leveraging isothermal amplification and single-strand conversion. Moreover, our platform outperforms the existing NASBA-based SDA sensors in terms of rapidity of workflow, while maintaining simplicity and sensitivity. CLASSIC also offers many advantages over qPCR such as shorter running times, simple operation, and label-free detection. One should be able to redesign target-binding arms of the hybridization probes and RPA primers, and readily apply CLASSIC to analyze various types of DNA biomarkers including antibiotic-resistant genes,<sup>25</sup> allele-specific single-nucleotide alterations,<sup>26</sup> and circulating tumor DNA (ctDNA).<sup>27</sup> Moreover, if an additional reverse transcriptase step were to become incorporated, CLASSIC could become utilized in viral RNA detection.<sup>28</sup> Future work may entail integrating universal primers<sup>29</sup> with additional light-up probe pairs to construct a multiplexed CLASSIC DNA detection platform.

## Author contributions

Jaekyun Baek: conceptualization, methodology, validation, formal analysis, data curation, visualization, writing – original draft preparation, review and editing. Jihyun Park: validation, writing – review and editing. Youngeun Kim: conceptualization, methodology, formal analysis, data curation, funding acquisition, project administration and supervision, writing – original draft preparation, review and editing.

## Data availability

All data generated or analyzed during this study are included in this published article (manuscript file) and its ESI.†

## Conflicts of interest

There are no conflicts to declare.

## Acknowledgements

This work was supported by the National Research Foundation of Korea (NRF) grant funded by the Korean government (MSIT) (No. 2022M3H4A1A04096393) and by the Creative-Pioneering Researchers Program through Seoul National University.

## References

- 1 B. Malorny, J. Hoorfar, C. Bunge and R. Helmuth, *Appl. Environ. Microbiol.*, 2003, **69**, 290–296.
- 2 M. E. Sengupta, M. Hellström, H. C. Kariuki, A. Olsen, P. F. Thomsen, H. Mejer, E. Willerslev, M. T. Mwanje, H. Madsen and T. K. Kristensen, *Proc. Natl. Acad. Sci. U. S. A.*, 2019, **116**, 8931–8940.
- 3 V. Vasioukhin, P. Anker, P. Maurice, J. Lyautey, C. Lederrey and M. Stroun, *Br. J. Haematol.*, 1994, **86**, 774–779.
- 4 E. Jergens, S. de Araujo Fernandes-Junior, Y. Cui, A. Robbins, C. E. Castro, M. G. Poirier, M. N. Gurcan, J. J. Otero and J. O. Winter, *Nanoscale*, 2023, **15**, 9390–9402.
- 5 S. Nayak, P. Kumar, R. Shankar, A. K. Mukhopadhyay, D. Mandal and P. Das, *Nanoscale*, 2022, **14**, 16097–16109.
- 6 J. M. Vindeirinho, E. Pinho, N. F. Azevedo and C. Almeida, *Front. Cell. Infect. Microbiol.*, 2022, **12**, 799678.
- 7 C. A. Heid, J. Stevens, K. J. Livak and P. M. Williams, *Genome Res.*, 1996, **6**, 986–994.
- 8 M. Parida, S. Sannarangaiah, P. K. Dash, P. Rao and K. Morita, *Rev. Med. Virol.*, 2008, **18**, 407–421.
- 9 I. M. Lobato and C. K. O'Sullivan, *TrAC, Trends Anal. Chem.*, 2018, **98**, 19–35.
- 10 T. Notomi, H. Okayama, H. Masubuchi, T. Yonekawa, K. Watanabe, N. Amino and T. Hase, *Nucleic Acids Res.*, 2000, **28**, e63–e63.
- 11 F. B. Dean, S. Hosono, L. Fang, X. Wu, A. F. Faruqi, P. Bray-Ward, Z. Sun, Q. Zong, Y. Du and J. Du, *Proc. Natl. Acad. Sci. U. S. A.*, 2002, **99**, 5261–5266.
- 12 Y. Zhao, F. Chen, Q. Li, L. Wang and C. Fan, *Chem. Rev.*, 2015, **115**, 12491–12545.
- 13 Y. Liu, Y. Li, Y. Hang, L. Wang, J. Wang, N. Bao, Y. Kim and H. W. Jang, *Nano Convergence*, 2024, **11**, 2.
- 14 J. A. Dwivedi-Yu, Z. J. Oppler, M. W. Mitchell, Y. S. Song and D. Brisson, *PLoS Comput. Biol.*, 2023, **19**, e1010137.
- 15 V. Narasimhan, H. Kim, S. H. Lee, H. Kang, R. H. Siddique, H. Park, Y. M. Wang, H. Choo, Y. Kim and S. Kumar, *Adv. Mater. Technol.*, 2023, **8**, 2300230.
- 16 G. Seyrig, R. D. Stedtfeld, D. M. Tourlousse, F. Ahmad, K. Towery, A. M. Cupples, J. M. Tiedje and S. A. Hashsham, *J. Microbiol. Methods*, 2015, **119**, 223–227.
- 17 O. Piepenburg, C. H. Williams, D. L. Stemple and N. A. Armes, *PLoS Biol.*, 2006, **4**, e204.
- 18 C. Kerr and P. D. Sadowski, *J. Biol. Chem.*, 1972, **247**, 311–318.
- 19 J. R. Sayers, W. Schmidt and F. Eckstein, *Nucleic Acids Res.*, 1988, **16**, 791–802.
- 20 W. E. Noteborn, L. Abendstein and T. H. Sharp, *Bioconjugate Chem.*, 2020, **32**, 94–98.
- 21 Y. Kim, A. B. Yaseen, J. Y. Kishi, F. Hong, S. K. Saka, K. Sheng, N. Gopalkrishnan, T. E. Schaus and P. Yin, *MedRxiv*, 2020.
- 22 Y. Zhang, B. Heym, B. Allen, D. Young and S. Cole, *Nature*, 1992, **358**, 591–593.
- 23 R. P. Connelly, P. F. Madalozzo, J. E. Mordeson, A. D. Pratt and Y. V. Gerasimova, *Chem. Commun.*, 2021, **57**, 3672–3675.
- 24 N. Kikuchi, A. Reed, Y. V. Gerasimova and D. M. Kolpashchikov, *Anal. Chem.*, 2019, **91**, 2667–2671.
- 25 N. A. Turner, B. K. Sharma-Kuinkel, S. A. Maskarinec, E. M. Eichenberger, P. P. Shah, M. Carugati, T. L. Holland and V. G. Fowler Jr, *Nat. Rev. Microbiol.*, 2019, **17**, 203–218.

- 26 M. Thorven, A. Grahn, K.-O. Hedlund, H. Johansson, C. Wahlfrid, G. R. Larson and L. Svensson, *J. Virol.*, 2005, **79**, 15351–15355.
- 27 M. Ignatiadis, G. W. Sledge and S. S. Jeffrey, *Nat. Rev. Clin. Oncol.*, 2021, **18**, 297–312.
- 28 A. Abd El Wahed, A. El-Deeb, M. El-Tholoth, H. Abd El Kader, A. Ahmed, S. Hassan, B. Hoffmann, B. Haas, M. A. Shalaby and F. T. Hufert, *PLoS One*, 2013, **8**, e71642.
- 29 K. Li, Y. Luo, K. Huang, Z. Yang, Y. Wan and W. Xu, *Anal. Chim. Acta*, 2020, **1127**, 217–224.